Spectroscopy and reactivity of size-selected Mg^+-ammonia clusters

James I. Lee,[a] David C. Sperry,[b] and James M. Farrar [c]
Department of Chemistry, University of Rochester, Rochester, New York 14627-0216

(Received 13 July 2004; accepted 11 August 2004)

Photodissociation spectra for mass-selected $Mg^+(NH_3)_n$ clusters for $n=1$ to 7 are reported over the photon energy range from 7000 to 38 500 cm^{-1}. The singly solvated cluster, which dissociates primarily via a N–H bond cleavage, exhibits a resolved vibrational structure corresponding to two progressions in the intracluster Mg^+-NH_3 modes. The addition of the second, third, and fourth solvent molecules results in monotonic redshifts that appear to halt near 8500 cm^{-1}, where a sharp feature in the electronic spectrum is correlated with the formation of a $Mg^+(NH_3)_4$ complex with T_d symmetry and the closing of the first solvation shell. The spectra for the clusters with 5 to 7 solvent molecules strongly resemble that for the tetramer, suggesting that these solvent molecules occupy a second solvation shell. The wavelength-dependent branching-ratio measurements show that increasing the photon energies generally result in the loss of additional solvent molecules but that enhancements for a specific solvent number loss may reveal special stability for the resultant fragments. The majority of the experimental evidence suggests that the decay of these clusters occurs via the internal conversion of the initially excited electronic states to the ground state, followed by dissociation. In the case of the monomer, the selective cleavage of a N–H bond in the solvent suggests that this internal-conversion process may populate regions of the ground-state surface in the vicinity of an insertion complex $H-Mg^+-NH_2$, whose existence is predicted by *ab initio* calculations. © *2004 American Institute of Physics.* [DOI: 10.1063/1.1802498]

INTRODUCTION

The cluster state of matter, consisting of weakly bound aggregates of atoms or of molecules bound by noncovalent forces, is widely viewed as a bridge from the gas phase to condensed phases. Ion solvation, unlike the other bulk properties of the condensed phase systems, can be probed in a size-dependent manner over a fairly narrow range of cluster sizes because of the short Debye length, the length scale over which neighboring ions in a solution are screened from one another.[1,2] Consequently, studies of the structures of small metal ion-solvent complexes and the size dependences of the dynamical processes occurring in those clusters have the potential to elucidate the properties of metal ions in the condensed phase.

Among the metal ion-solvent systems that have been probed size selectively by spectroscopy, solvated alkaline-earth cations are among the most interesting, particularly from the perspective that more than one oxidation state of the metal may be involved in the photochemistry.[3] The singly charged alkaline-earth ions, e.g., Mg^+, Ca^+, and Sr^+, do not occur naturally in condensed phase systems but nonetheless provide insight into the ion-molecule interactions that ultimately lead to solvation through the electronic transitions of the single valence electron in these species. The coupling of the electronic energy of the atomic ion core with reactive processes involving solvent degrees of freedom[4–6] provides critical opportunities for probing the structural and dynamical features of the solvation process.

Previous studies from a number of laboratories have shown consistent spectroscopic motifs in alkaline-earth cations solvated by polar solvents: as the cluster size increases, the metal-centered transitions become redshifted, reaching a maximum at a relatively small number of solvent molecules.[7–12] In early work on systems based on Sr^+, this observation was interpreted by Bauschlicher *et al.*[13] in terms of destabilization of the ground state by metal-ligand repulsions. In previous publications, we suggested that with increasing cluster size, the energy required to remove the valence electron in Sr^+ and create an ion pair may be compensated for by attractions that arise from solvating the oppositely charged constituents of such a system.[14,15] However, that interpretation was clouded by the role that the $4d$ states of Sr^+ played, particularly as the ligand field mixed these low-lying states into the allowed $5s$-to-$5p$-type transitions of the large clusters.

A full understanding of these processes requires a theoretical interpretation in the form of *ab initio* calculations that find structures, vertical transition energies, and transition moments.[13,16] Cluster systems based on Mg^+ are particularly attractive because of the relatively small number of electrons and the inaccessibility of $3d$ orbitals to low-lying electronic states of clusters. A very recent exploratory calculation on $Mg^+(H_2O)_n$ clusters suggests that electron-density redistribution has a size dependence, and evidence for the formation of solvated ion-pair states in clusters with as few as six solvent molecules has been presented.[17–20]

The $Mg^+(NH_3)_n$ system has been the subject of several

[a]Present address: Stanford Research Systems, 1290 D Reamwood Avenue, Sunnyvale, CA 94089.
[b]Present address: Pfizer Research Laboratories, 7000 Portage Road, Mail Stop 4831-259-175, Kalamazoo, MI 49001.
[c]Author to whom correspondence should be addressed. Electronic mail: farrar@chem.rochester

experimental and theoretical studies. The earliest *ab initio* calculations on this system[13,21] predicted the ground- and excited-state geometries and vibrational frequencies, excitation energies, and band intensities for clusters with up to three solvent molecules. More recent studies were concerned with the energetics and kinetics of ligation, especially for the larger clusters. Milburn *et al.*[22] presented studies on the ammonia ligation kinetics of bare Mg^+ and Mg^+ bound to c-C_5H_5, focusing on clusters with four or fewer NH_3 molecules. The ligation rates indicated that the fourth solvent was bound much less strongly than the third, leading the authors to suggest that it was present in a second solvation shell. The density functional theory (DFT) calculations characterized both tetrahedral complexes in which four solvents were bound directly to the metal in a first solvation shell, denoted here as (4+0), and clusters denoted (3+1), in which the first three ligands were bound to the metal in a C_3 geometry with the fourth solvent in a second shell. At the level of theory employed for these calculations, it was not possible to predict which structure was of the lowest energy. The collision-induced dissociation measurements of the bond energies in the $Mg^+(NH_3)_n$ system were reported by Andersen *et al.*[23] along with the supporting DFT results indicating that the (4+0) and (3+1) complexes, the former having a square planar geometry rather than a tetrahedral, were so close in energy as to prohibit a robust prediction of the most stable ground-state structure. The photoionization studies of the $Mg(NH_3)_n$ clusters in combination with the *ab initio* calculations led to similar conclusions.[24]

More recently, experimental studies of the photodissociation spectroscopy of $Mg^+(NH_3)_n$ clusters with up to four solvent molecules as well as the *ab initio* calculations of the ground- and excited-state geometries and energies and electronic transition moments have been reported by Yoshida and co-workers.[25,26] Consistent with other alkaline-earth-polar solvent systems, the optical spectra exhibited large redshifts with increasing cluster size. The DFT calculations applied to the ground and excited electronic states of these clusters yielded estimates for the $\langle r^2 \rangle$ and $\langle z \rangle$ moments of the valence electron distributions. These moments indicated that a significant contribution to the size-dependent redshift of these clusters arose from the diffusion of the valence electron away from the atomic ion center in a single-center ion-pair state. These studies emphasized the evolution of the solvent shell structure as a function of the cluster size, addressing the possibility of electron delocalization away from the metal center, particularly in the excited states of the larger clusters in the size range examined.

In the present paper, we report a study of the photodissociation spectra of the first seven clusters of Mg^+ solvated by ammonia molecules. The clusters are demonstrably colder than those in the study of Yoshida and co-workers[25,26] and provide clear evidence of the appearance of an especially stable isomer of tetrahedral symmetry at $n=4$. The dominant transitions of the clusters with $n \geqslant 5$ are shown to be based on this tetrahedral core. In addition, the branching ratios for the full size range of all the clusters are reported.

EXPERIMENT

The experimental apparatus for these experiments has been described in detail in previous publications;[9] only a summary is presented here. The clusters are produced in an ion source in which a gas mixture of 30% ammonia seeded in He is expanded adiabatically through a solenoid-driven pulsed valve (General Valve, Series 9) into a rotating rod-type[27] laser vaporization source. Magnesium metal (Alfa-Aesar, 99.8%) is ablated and ionized by focused second harmonic radiation from a Nd^{3+}:YAG laser (Continuum, NY-61). The seeded vapor is forced through the Mg^+ plasma, creating a distribution of cluster sizes of the form $Mg^+(NH_3)_n$. The clusters are collisionally cooled as they travel down a source block channel and expand supersonically into the source chamber, which is held at a pressure of 10^{-5} torr during the experiment. They then enter the extraction region of a Wiley-McLaren-type time-of-flight mass spectrometer.[28] The clusters reach a mass-independent spatial focus 1.5 m downstream from the center of the extraction region. The clusters are photolyzed by radiation, which transversely intersects the cluster beam at the spatial focus.

Radiation is provided by a narrow bandwidth ($\sim$0.2 cm^{-1}) singly resonant optical parametric oscillator (OPO) (Spectra Physics, MOPO-730). The OPO is pumped by the third harmonic of an injection seeded Nd^{3+}:YAG laser (Spectra Physics, GCR-190) running at 10 Hz. The OPO signal wave tuning range is from 440 to 690 nm and its idler wave tuning range is from 730 to 1830 nm. The OPO is also equipped with a frequency doubling option (FDO-900), which converts the oscillator output into an ultraviolet radiation. Photodissociation creates a distribution of product and unphotolyzed reactant ions which are separated using a reflectron-type mass spectrometer. A set of off-axis microchannel plates detects and amplifies the signal. The data are received by a transient recorder (DSP, 2100AS), typically averaged over 100 laser shots (DSP, 4101), and sent from the CAMAC crate to a PC. The photochemical product or ''daughter'' ions are produced from a single ''parent'' cluster ion and are normalized to the integrated intensity of the unattenuated parent. The photodissociation pulse energy is monitored throughout the experiment and kept at a constant value of 1 mJ/pulse with a spot size with a diameter of 5 mm. The Power dependence studies on the product channels have shown a linear response in this photodissociation power regime.

RESULTS

The laser vaporization source produces a distribution of clusters that depends on the operating conditions. Under the moderate expansion conditions that we employ, the formation of adequate intensities of clusters with up to seven solvent molecules was achieved readily. Clusters incorporating all three of the naturally occurring isotopes of Mg, i.e., ^{24}Mg, ^{25}Mg, and ^{26}Mg were formed, and the time structure of the ion packets allowed us to perform dissociation experiments with the clusters containing the most abundant ^{24}Mg isotope. The clusters sizes containing four or more solvents also exhibited hydrogen-atom loss from the N–H bond cleavage in

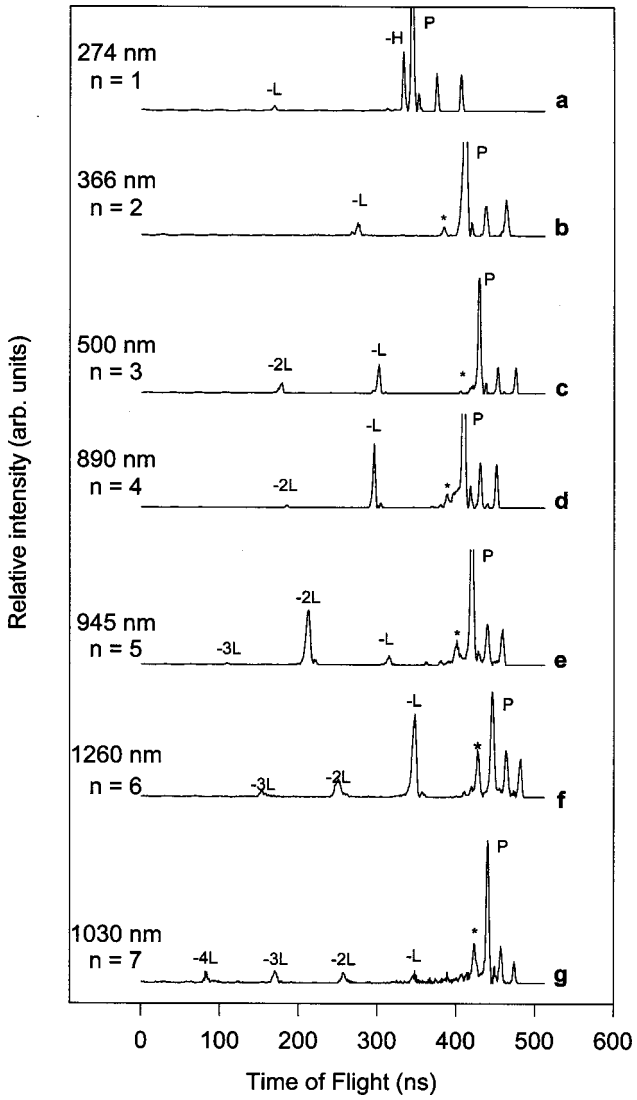

FIG. 1. Photodissociation mass spectra for $n=1$ to 7 clusters at indicated wavelengths. Asterisks in the $n=2$ to 7 spectra mark parent ions that have undergone hydrogen-atom loss in the absence of the photodissociation laser.

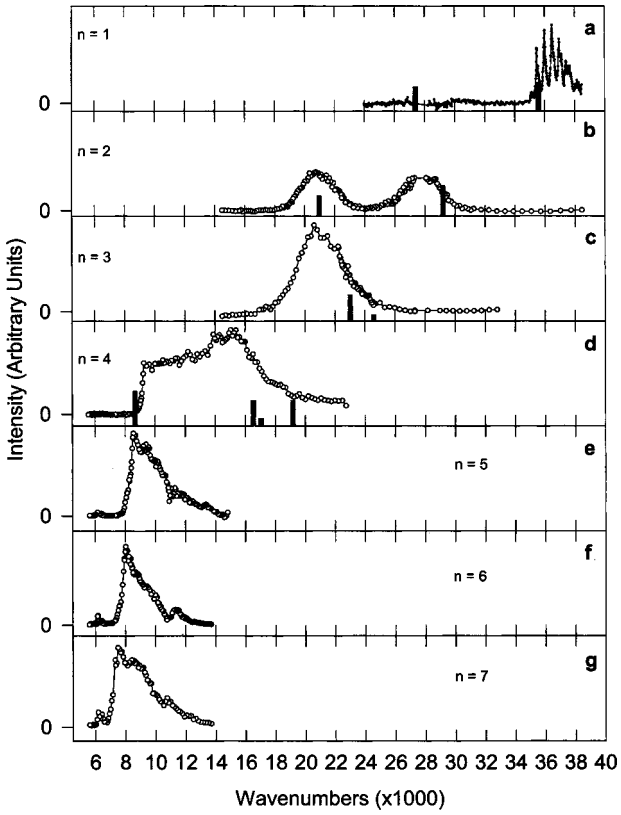

FIG. 2. Total photofragmentation spectra for $Mg^+(NH_3)_n$, for $n=1$ to 7. Vertical bars in the spectra for $n=1$ to 4 give theoretical positions of transitions computed by Yoshida *et al.* [Ref. 26]. The heights of the bars are proportional to the oscillator strengths.

the ground electronic state. The extent of this H-atom loss was significantly less than that observed in $M^+(H_2O)_n$ (Refs. 11, 12, and 29) and $M^+(CH_3OH)_n$,[30–33] with M=Mg, Ca, and Sr, where the parent-ion distributions were dominated by "product switching," in which the most abundant parent ions appeared to be solvated metal hydroxide cations, $MOH^+(H_2O)_m$, for cluster sizes as small as four to six solvent molecules.

A group of daughter-ion mass spectra for the $Mg^+(NH_3)_n$ clusters with $n=1-7$ is shown in Fig. 1. We will use the shorthand notation shown in that figure to refer to the product channels. Figure 1(a) shows the daughter-ion mass spectrum of $n=1$, the monomer. Note that this is the only spectrum where $-H$ is observed after photoexcitation. Panels b–g in Fig. 1 each show that as the cluster size increases, so does the possibility of losing more than one ligand upon photodissociation. In Fig. 1(g), the daughter-ion mass spectrum for the $n=7$ cluster shows that it is possible to eliminate 1, 2, 3, or 4 ligands. This is consistent with calculations that show the successive ligand binding energies decrease with the increasing cluster size[13,30] and with the idea that the larger clusters retain more internal energy,[34,35] thereby decreasing the effective endothermicity of the ligand-loss channel.

PHOTODISSOCIATION SPECTROSCOPY

The total photodissociation spectra for $Mg^+(NH_3)_n$ for $n=1$ to 7 are plotted in Fig. 2. Here, we summarize the results for each cluster size, beginning with the monomer. In qualitative agreement with Yoshida *et al.*[25] and as indicated in Fig. 1(a), the dissociation of the monomer proceeds almost exclusively ($\geqslant$90%) via the $-H$ channel. We are unable to observe the NH_3^+ products formed by dissociative charge transfer. The monomer spectrum consists of a single strong band with an origin at 35 400 cm^{-1} and a progression in the vibrational modes in the excited electronic state. We also located an extremely weak signal near 28 500 cm^{-1}, but the total photodissociation signal recorded never exceeded 1% of the most intense band. Despite a careful search, we were unable to find a band of intensity comparable to the one at 36 000 cm^{-1}. The general features of the spectrum observed in Fig. 2(a) and the electronic origin are in agreement with that reported by Yoshida *et al.* and with the *ab initio* calculations reported in that work as well as earlier calculations reported by Bauschlicher *et al.* The intense band beginning at 35 400 cm^{-1} is attributed to the excitation of the $2\,^2A_1$ state of $Mg^+(NH_3)$ based on the $3p\sigma$ orbital, for which the

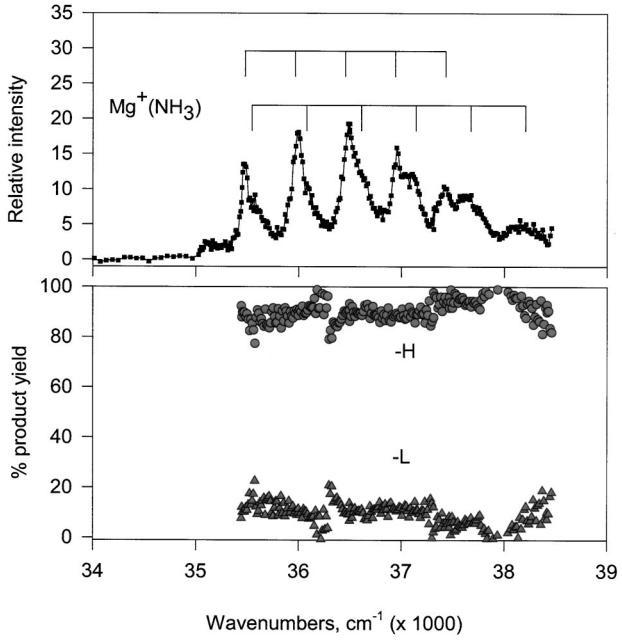

FIG. 3. Expanded scale version of the photofragment spectrum for the $2\,^2A_1$ band of the $Mg^+(NH_3)$ cluster. The upper and lower brackets indicate the vibrational progressions at 488 and 524 cm^{-1}, as discussed in text.

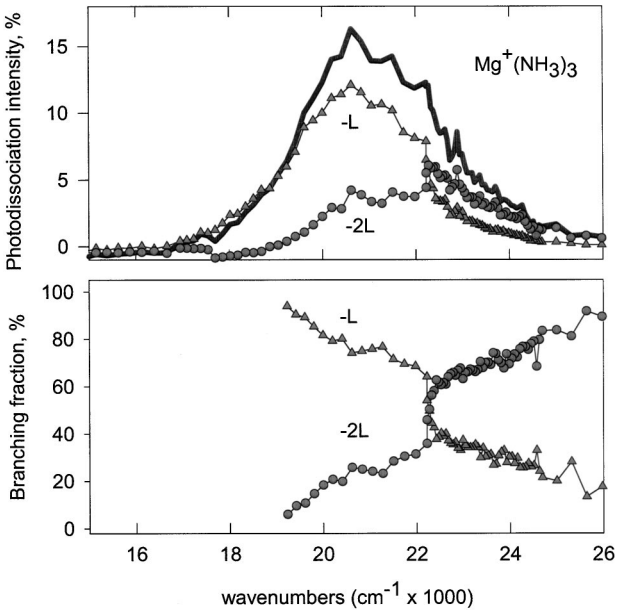

FIG. 4. Upper panel: total fragmentation signal (solid curve) for $Mg^+(NH_3)_3$, with contributions from each fragment channel. Lower panel: branching ratios for major fragments vs photolysis frequency.

calculations by Yoshida *et al.*[25] and by Bauschlicher *et al.*[13] predict origins at 38 150 and 39 150 cm^{-1}, respectively. The weaker band we observe at 28 500 cm^{-1} also agrees in intensity and position with the observations of Yoshida *et al.* and is within 1700 cm^{-1} of the predictions of both sets of *ab initio* calculations for the origin of the $1\,^2E$ state. However, the calculations both predict that the intensity of this transition is of a comparable magnitude to that for the observed $2\,^2A_1$ band. At present, there is no satisfactory explanation for this intensity anomaly although it has been observed in other Mg^+ systems.[36,37]

As the monomer spectrum shows in Fig. 2(a), we are able to resolve vibrational structure. Figure 3 shows the monomer photodissociation data on an expanded scale, indicating two Franck-Condon progressions of the vibrational transitions in the excited electronic state. One progression is much stronger than the other and has a smaller vibrational spacing. As the photolysis frequency decreases, the progressions begin to overlap. To the best of our knowledge, there are no vibrational frequency calculations for $Mg^+(NH_3)$. However, because the bonding in $Mg^+(NH_3)$ and $Mg^+(H_2O)$ is similar[13] and their reduced masses are comparable, it is possible to make a tentative vibrational assignment by comparison to existing vibrational calculations on $Mg^+(H_2O)$ (Ref. 16) and $Sr^+(NH_3)$.[38] The vibrational spacing of the strong progression is about 488 cm^{-1}, whereas the weak progression's frequency is about 524 cm^{-1}. According to Sodupe and Bauschlicher, there are only two modes that are of similar frequency in the $2\,^2A_1$ excited electronic state of $Mg^+(H_2O)$.[16] These modes are the Mg^+-O stretch and the out-of-plane wag at 484 and 403 cm^{-1}, respectively. In $Sr^+(NH_3)$, only the NH_3 tilt is of similar frequency (roughly 500 cm^{-1}) to the spacing we observe.[38] We therefore tentatively assign the strong progression as the Mg^+-N stretch and the weak progression as the NH_3 tilt, which is roughly analogous to the wags in $Mg^+(H_2O)$.

The photodissociation spectrum for the dimer, $Mg^+(NH_3)_2$, is shown in the second panel of Fig. 2. The peak positions in the spectrum are in good agreement with the experimental and theoretical results reported by Yoshida *et al.*, although the intensity of the lower energy peak reported here is approximately twofold higher. Both excited states are ^2B species in C_2 symmetry. The predominant product in both bands corresponds to the loss of a single ligand, denoted as $-L$. The H-atom loss channel is absent in the dimer. The electronic band peak of $p\sigma$ character shifts from $\sim$36 500 cm^{-1} in the monomer to $\sim$28 000 cm^{-1} in the dimer. This corresponds to more than a 1-eV shift to the red. Given our estimate of the endothermicity for H loss in the monomer, it is quite probable that these photolysis energies are below the threshold for any reaction but ligand loss. This situation is perpetuated as the redshift continues with increasing cluster size. Thus, only the monomer chromophore, whose oscillator strength is in the ultraviolet region of the spectrum, allows $-H$ to occur.

The photodissociation spectrum for the trimer, $Mg^+(NH_3)_3$, is shown in more detail in the upper panel of Fig. 4. Although qualitatively like that reported previously by Yoshida *et al.*, the signal-to-noise ratio is significantly better in this study. The $1\,^2E \leftarrow 1\,^2A_1$ excitation can be correlated with the intensity maximum at 21 000 cm^{-1}. The *ab initio* calculations also predict that the $2\,^2A \leftarrow 1\,^2A$ transition should be found approximately 1600 cm^{-1} above the energy of the first excited state. Although the data in the previous study were not of a high enough signal-to noise-ratio to allow that assignment to be made unambiguously, the present study does show a shoulder in the data near 22 300 cm^{-1}, in the correct region of the spectrum for excitation of the $2\,^2A$ state. The branching ratios for dissociation in $Mg^+(NH_3)_3$,

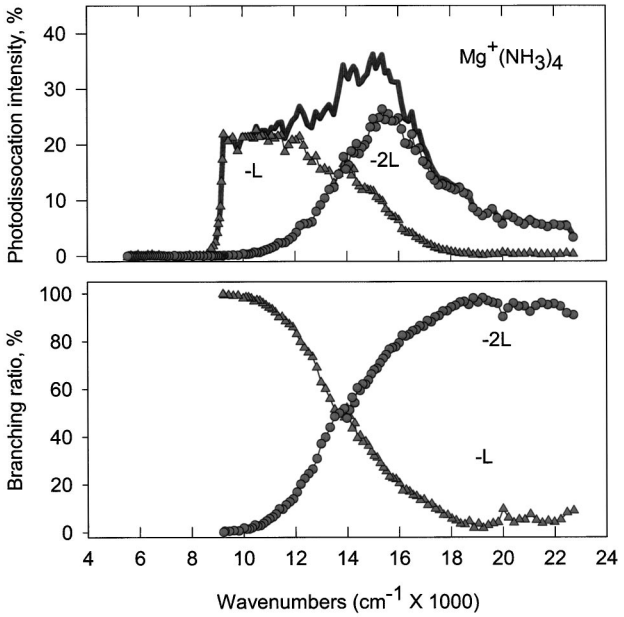

FIG. 5. Upper panel: total fragmentation signal (solid curve) for $Mg^+(NH_3)_4$, with contributions from each fragment channel. Lower panel: branching ratios for major fragments vs photolysis frequency.

shown in the lower panel of Fig. 4, make that assignment even clearer. These data for the product branching are quite different from those reported in the previous study, in which the -2L channel was shown to dominate the single solvent loss channel $-$L over the entire wavelength range. Figure 4 shows that in the low-frequency region of the spectrum, the $-$L channel is most intense but is attenuated at higher frequency, as the -2L channel dominates the dissociation. The branching ratio shows a very clear point of inflection at 22 300 cm^{-1}, precisely where the shoulder in the total dissociation data appears. It is not unreasonable to expect that in the dissociative events occurring through excited electronic state surfaces, the fragmentation pattern should depend sensitively on the electronic state. The clear bias in favor of the -2L channel that appears at 22 300 cm^{-1} is consistent with the excitation to a new electronic state. The branching-ratio data strengthen the assignment of this excitation to the $2\,^2A \leftarrow 1\,^2A$ transition.

The experimental data for the dissociation of $Mg^+(NH_3)_4$ are shown in more detail in the top panel of Fig. 5. They suggest that the behavior of this cluster is transitional between that of the smallest clusters, which show consistent redshifts with increasing size, and the largest clusters, which appear to have a common spectral element. The clusters with four solvent molecules appear to have at least two separate components in their spectra, and the DFT calculations have provided a rationalization for this behavior. The data shown in Fig. 5 are qualitatively consistent with those of Yoshida *et al.*, although the sharpness of the spectral features is accentuated in the present study. In $Mg^+(NH_3)_4$, the higher energy band near 16 000 cm^{-1} appears to evolve from the broad feature observed in the trimer. Yoshida *et al.* show that two possible ground-state cluster structures, one having a sawhorse or a distorted square planar structure with C_{2v} symmetry and a second with four solvents tetrahedrally arranged around the metal center, are essentially isoenergetic. Despite the near degeneracy of the ground-state energies of the two dominant configurations, the calculated energies of the excited states arising from these two different geometries have very distinct behaviors. The calculations confirm that the higher energy band originates from clusters with C_{2v} symmetry and appears as a redshifted version of the dominant band in the triply solvated cluster. A second transition in the quadruply solvated cluster at much lower excitation frequencies has a sharply rising edge near 7000 cm^{-1}, which reaches a plateau and blends into the tail of the higher energy transition. The calculations of Yoshida *et al.* show clearly that the lower energy transition belongs to clusters with tetrahedral symmetry. The most striking characteristic of such a transition arises from the fact that the $3p$ orbitals on Mg^+ are degenerate in a ligand field of T_d symmetry, causing the electronic states based on the $3p \leftarrow 3s$ atomic transitions to be quasidegenerate.

Both of these clusters have four solvents bound to the metal and are therefore denoted as $(4+0)$. Yoshida *et al.* also suggested that other geometries were energetically accessible but no solid evidence for their participation was found in the experimental data. In particular, clusters having a $(3+1)$ structure, in which the fourth solvent molecule is the second solvation shell in a hydrogen-bonded configuration that bridges the two first solvation shell molecules, have been suggested as playing an important role in the tetramer. However, the electronic transition energies calculated for such species only have significant oscillator strength in the region above 20 000 cm^{-1}, well to the blue of the dominant absorptions.[26]

Both panels of Fig. 5 also show the product selectivity of the fragmentation patterns observed in the two distinct peaks that contribute to the total dissociation signal. The branching-ratio data in the lower panel of Fig. 5 show that the lower energy band results almost exclusively from the loss of a single ligand, whereas the higher energy band is dominated by the -2L channel.

The spectra for the pentamer, hexamer, and heptamer, shown in detail along with their fragmentation patterns in Figs. 6–8, reveal a clear relationship to the data for the tetramer. Each of those spectra shows that the lowest energy feature appears to be fairly narrow; a series of partially resolved shoulders and peaks occurring at higher photon energies cannot be assigned definitively, but those features are likely to be associated with other structural isomers. In a tetrahedral ligand field, the $3p$ orbitals of Mg^+ remain degenerate, leading to the narrow absorption observed. The fact that the general shapes of the spectra for the larger clusters strongly resemble that deduced for the lowest energy feature in the tetramer suggests that the first solvation shell fills in $Mg^+(NH_3)_4$ and that the tetrahedal geometry forms the most stable core for the second solvation shell.

The branching-ratio data provide additional insight into the dissociation processes in these clusters. In Fig. 5 for $Mg^+(NH_3)_4$, the loss of a single ligand dominates the low-energy side of the spectrum. As the photolysis energy increases, $-$L competes less effectively with -2L until their

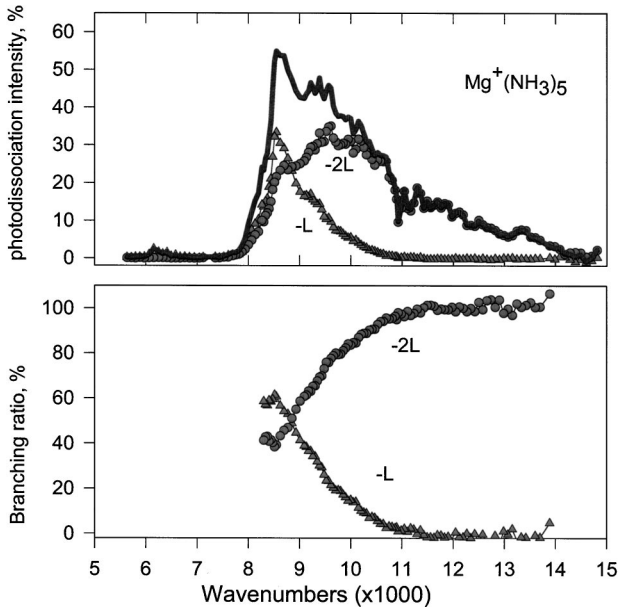

FIG. 6. Upper panel: total fragmentation signal (solid curve) for $Mg^+(NH_3)_5$, with contributions from each fragment channel. Lower panel: branching ratios for major fragments vs photolysis frequency.

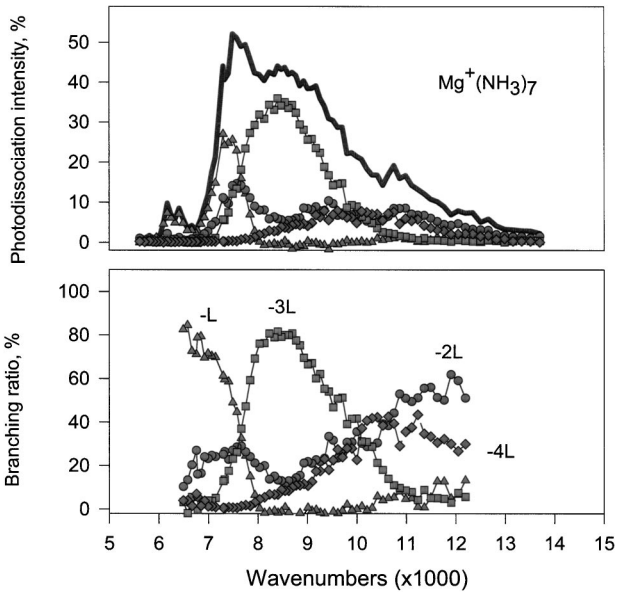

FIG. 8. Upper panel: total fragmentation signal (solid curve) for $Mg^+(NH_3)_7$ with contributions from each fragment channel. Lower panel: branching ratios for major fragments vs photolysis frequency.

roles are reversed and $-2L$ is the dominant channel. This trend repeats as the cluster size increases. For example, in the data for $Mg^+(NH_3)_5$ dissociation shown in Fig. 6, $-L$ dominates at low photolysis energies and $-2L$ dominates at high photolysis energies. As the photolysis frequency increases, the probability of eliminating multiple solvent ligands also increases. Figure 7 for $Mg^+(NH_3)_6$ shows that the channels of $-L$, $-2L$, and $-3L$ are "switched on" as the photolysis energy increases. This is easily understood in terms of the reaction enthalpies. Solvation lowers the ligand-loss threshold,[13,39,40] allowing multiple ligand loss to occur.

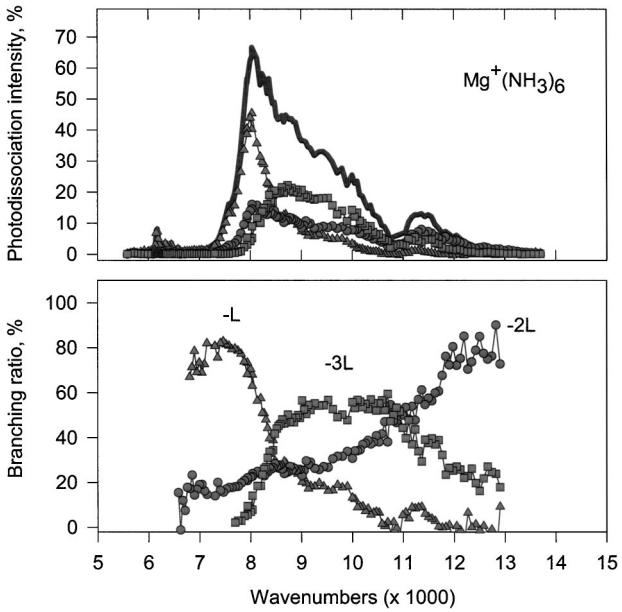

FIG. 7. Upper panel: total fragmentation signal (solid curve) for $Mg^+(NH_3)_6$ with contributions from each fragment channel. Lower panel: branching ratios for major fragments vs photolysis frequency.

Eliminating multiple ligands requires more energy than eliminating a single ligand; thus, the multiligand loss channels appear at higher photolysis energies.

A closer look at the nature of the photofragments that contribute to the spectral intensities suggests that the fragmentation patterns are more complex than a simple stepwise increase in the number of evaporated solvent molecules with increasing photon energy. Comparing Figs. 6 and 7 shows that the dominant shoulders on the high-energy side of the dissociation spectra for the $n=5$ and 6 clusters correspond to formation of the trimer ion, $Mg^+(NH_3)_3$, in both cases. This suggests that the higher energy features may arise from parent-ion clusters with $(3+2)$ or $(3+3)$ structures, respectively. Similarly, the major shoulder to the blue of the origin of the $Mg^+(NH_3)_7$ spectrum corresponds to the loss of three solvent molecules to form the tetramer. However, at higher photolysis energies, this channel is attenuated and $-2L$ and $-4L$ channels dominate the dissociation.

DISCUSSION

A large body of experimental data, such as those reported here by photodissociation of cationic clusters as well as other experimental and theoretical studies on isoelectronic systems, all focus on the nature of the interaction of the valence electron of the cluster core with the electrostatic field created by the solvent system. The consistent redshifts exhibited by the absorption spectra of such metal-solvent clusters based on the effective one-electron cores and their size dependences provide fundamental information about the solvation phenomenon. A particularly salient point in the present study is the solvent dependence of the cluster size at which the redshift appears to saturate. Roughly speaking, large redshifts require direct core-solvent interactions, and thus, the saturation of the redshift provides information about the solvent shell closing. In $Mg^+(NH_3)_n$, the redshift satu-

rates in the infrared region of the spectrum for clusters with a first solvation shell containing four solvent molecules. In contrast, the studies from the laboratory of Misaizu *et al.* on $Mg^+(H_2O)_n$ (Ref. 29) and from our laboratory on $Mg^+(CH_3OH)_n$,[33] both of which are built on strongly hydrogen-bonded solvents, show that the redshift saturates for three molecules. The experimental work by Lisy[41] and by Stace[1] suggests that in strongly hydrogen-bonded solvents, charge enhancement results in binding energies for the second solvation shell species that are comparable to those for solvents bound directly to the central ion. Thus, in strongly hydrogen-bonded systems, fewer molecules are required to close the first solvation shell.

Size-dependent trends in the evolution of the electronic spectra of the cluster systems provide some of the most incisive probes of solvation phenomena. Estimates of the moments of the valence electron distributions in clusters have been shown to be important metrics for the development of the delocalized states that precede spontaneous ionization and solvated electron formation.[15,42] Conventional oscillator strength sum rules provide experimental probes of the ground-state properties such as $\langle r^2\rangle^{\frac{1}{2}}$,[43] whereas *ab initio* calculations may be employed to estimate the radial electron-density distributions and their moments both in the ground and excited states. The size-dependent growth in $\langle r^2\rangle^{\frac{1}{2}}$ has contributions from the metal-ligand repulsions that ''squeeze'' the electron out of the volume occupied by the solvent molecules, as well as from the interactions that drive the electron into a spherically symmetric one-center ion-pair Rydberg state. Yoshida *et al.*[26] show that the former contributions can be assessed by evaluating $\langle z\rangle$, the spatial extent of the electron-density distribution along a symmetry axis of the cluster, for the singly occupied molecular orbital (SOMO). The result of this analysis shows that in the tetrahedral $Mg^+(NH_3)_4$, $\langle z\rangle=0$, demonstrating that the expansion of the electron density is spherically symmetric, arising from the growth of the one-center ion-pair character of the cluster. The analysis also shows that the values of $\langle r^2\rangle^{\frac{1}{2}}$ for the excited states of the $n=3$ and 4 clusters based on the $3p$ orbitals of Mg^+ are almost twice the size of the ^2P state of the bare ion. The authors attribute this behavior to increased charge-transfer character in the excited states, as observed in the solvation of alkali atoms.[44–46] This increased charge-transfer character in the excited states of $Mg^+(NH_3)_n$ for $n>2$ leads to a stronger binding in the excited states of the larger clusters, thus increasing the absorption redshifts.

By removing the effects of the *d-p* mixing, the $Mg^+(NH_3)_n$ systems confirm that the redshifts seen in the dissociation spectra of the larger clusters arise from increasing ion-pair character of the ground- and excited-state wave functions. The same spectroscopic motif is seen in the two isoelectronic analogs, suggesting that common issues in electronic structure are responsible for this behavior. The first of these is the $Na(NH_3)_n$ system reported by Hertel *et al.*,[47] in which complete absorption spectra have been obtained for clusters with up to six solvent molecules. The earliest theoretical treatments of the $Na(NH_3)_n$ system[48,49] were mounted to help understand size-dependent ionization potential measurements. Most pertinent to the comparison between neutral clusters based on the Na core and ionic clusters built around Mg^+ is the idea that the most stable structures for the first four $Na(NH_3)_n$ clusters are interior structures that maximize the number of Na–N interactions.[49] Although the specific details of the size-dependent redshift motif differ in detail with those observed in $Mg^+(NH_3)_n$, large shifts that occur during the filling of the first solvation shell decrease significantly in magnitude as the fifth and sixth solvents, which do not interact directly with the atomic core, are placed in a second solvation shell. Reminiscent of the narrowing of the absorption band in $Mg^+(NH_3)_4$ clusters with T_d symmetry, the metal-solvent absorption decreases in width from $\sim$1500 cm^{-1} in the $n=3$ cluster to 700 to 1000 cm^{-1} in the larger clusters. However, only a single structure of D_{2d} symmetry is proposed for the lowest energy state of the tetramer. Such a structure provides a ligand field that partially lifts the degeneracy of the $3p$ orbital set on Na, and therefore does not predict a narrow low-energy metal-centered transition like that observed for the $n=4$ to 7 $Mg^+(NH_3)_n$ clusters.

A second isoelectronic analog, in which the effective one-electron core also has vibrational structure, is the system $NH_4(NH_3)_n$ based on the Rydberg molecule NH_4, which is isoelectronic with Na. The photodepletion spectra for the clusters $NH_4(NH_3)_n$, with $n=1$ to 8 (Refs. 50 and 51) show a remarkable resemblance to spectra of the isoelectronic species $Na(NH_3)_n$ and $Mg^+(NH_3)_n$. The *ab initio* calculations[51,52] provide rigorous assignments that confirm the analogies in the structures and the spectra. The spectral width of the band in the $n=4$ cluster is at least a factor of 2 narrower than that of the preceding cluster and reflects the fact that the tetrahedral geometry of the $n=4$ ligand field allows all the excited components of the $3p\,^2F_2$ state to remain degenerate. Unlike $Mg^+(NH_3)_4$, in which the spectrum shows evidence for isomers of C_{2v} and T_d symmetry, the structure of the ammonium radical core provides a unique tetrahedral environment around which the ligands bind. The similarity of the spectra for the $n=5$ to 8 clusters is consistent with the closing of the first solvation shell with four solvents.

The similarities of the spectra for the isoelectronic species $Mg^+(NH_3)_n$, $Na(NH_3)_n$, and $NH_4(NH_3)_n$ are no coincidence, and theoretical calculations suggest that two important factors are at work in establishing this common spectral motif: the first solvation shell fills in all three cases when four solvent molecules bind to the core, and the electronic transitions are $3p\leftarrow 3s$ in character. In the case of $Na(NH_3)_n$, dissociative photodepletion measurements and probes of the bound-state structure based on photoelectron spectroscopy in $Na^-(NH_3)_n$ (Ref. 53) confirm the compression of the bound energy-level structure with increasing the cluster size. The strong redshift that occurs as the first solvation shell fills reflects the role that the solvent molecules play in driving the valence electron into a SOMO that is increasingly diffuse.

One final spectral feature in the largest clusters that requires explanation and may hold additional information

about the solvation process begins to appear in $Mg^+(NH_3)_5$ as a weak absorption near 6100 cm^{-1}. This weak band is accessed at the same frequency in each of the clusters $Mg^+(NH_3)_{5-7}$ and is enhanced in intensity as n increases. This feature does not redshift with increasing the cluster size, and it is separate from the band we assign to the electronic $3p \leftarrow 3s$-like transitions of the metal. This suggests that the transition may not be metal centered. Brockhaus *et al.* observe a strong peak near 6300 cm^{-1}, which they assign to the vibrational combinations or overtones within the ammonia ligands.[47] Their principal proof of this assignment lies in examining $Na(NH_3)_8$ and $Na(ND_3)_8$ together. Their data show a well-separated pair of spectral peaks in the deuterated cluster, and the lower energy peak qualitatively corresponds with the expected shift in vibrational energies caused by deuteration. However, they do not observe an increase in intensity with cluster size. Rather, their data show that the intensity of this transition decreases with additional ligands. A comparison with the deuterated analogs $Mg^+(ND_3)_{5-7}$ may allow us to make definitive statements on whether this band is caused by a ligand-centered chromophore as argued by Brockhaus *et al.*[47]

Among the $Mg^+(NH_3)_n$ cluster systems, the singly solvated species is unique in undergoing photodissociation primarily via hydrogen-atom loss. Our experimental data indicate that approximately 90% of the products from the photodissociation of $Mg^+(NH_3)$ are detected as the metal-amide $MgNH_2^+$ species, independent of the photolysis wavelength. This result is qualitatively similar to that reported by Yoshida *et al.*,[25] although these authors reported a slightly smaller branching fraction of 70%. The *ab initio* calculations by Bauschlicher *et al.* yield a value of 1.65 eV (38 kcal/mol) (Ref. 13) for the endothermicity of the ligand evaporation channel; estimating the H-loss reaction enthalpy requires a knowledge of the Mg–N bond strength in Mg^+NH_2. Clemmer and Armentrout have investigated the bond energies of several M^+NH_2 systems, where M is a transition metal.[54] In studies with Ni and Co, the metal-amide bonds appear to be covalent, and are approximately 0.19 and 0.11 eV stronger than the corresponding metal–ammonia bonds, respectively. Thus, from the N–H bond strength in NH_3 (109 kcal/mol) and the estimated difference in the bond strengths of the M^+NH_3 and M^+NH_2 systems,[54] a reasonable estimate for the endothermicity of the H-atom-loss channel is roughly 104 kcal/mol, approximately 66 kcal/mol larger than for ligand loss. The appearance of H-loss products in the lower energy band reported by Yoshida *et al.* suggests that the parent ions are vibrationally excited.

The dominance of the H-loss channel over the ligand-loss channel in $Mg^+(NH_3)$ is counterintuitive, especially when one considers that the ligand-loss channel is substantially less endothermic than N–H bond cleavage, and the latter process likely occurs over a potential barrier in excess of its substantial endothermicity. The high selectivity of the dissociation process raises the question of whether bond cleavage occurs on the ground- or on the excited-state surface. In the related $Mg^+(CH_3OH)$ system,[33,55] the exclusive formation of $MgOH^+$ in the monomer led us to propose an excited-state model for product formation. The absence of any significant vibrational structure in the photodissociation action spectrum was attributed both to the short excited-state lifetime and the high density of torsional levels in the cluster.

There is experimental and theoretical evidence to support an insertion pathway for the hydrogen-atom-loss (−H) channel in the $Mg^+(NH_3)$ system. Of particular interest is the fact that the density functional theory calculations by Milburn *et al.* locate a stable minimum on the ground-state surface for Mg^+NH_3 with an insertion structure $H–Mg^+NH_2$ that lies 51 kcal/mol above the C_{3v}-symmetric global minimum assigned to the electrostatically bound complex.[22] Experimentally, similar insertion complexes, such as $H–CoNH_2^+$, have been detected directly by Clemmer and Armentrout,[54,56] who estimated that the lifetime of such a species must be at least 60 μs and attributed that stability to a potential well 0.8 eV in depth. However, these observations are compatible with ground-state insertion.

The fact that the branching ratio for H loss versus ligand evaporation is essentially flat over the entire $2\,^2A_1$ band is consistent with dissociation on the ground-state surface following internal conversion from excited states, as has been discussed by Fuke and co-workers in the context of this[25] and other solvated Mg^+ systems.[10,29,57] However, the "bond-stretching attraction" model that has been advanced to describe such electronic-to-vibrational energy-transfer processes[58] does not readily address the manner in which nonstatistical decay by H-atom loss dominates the less-endothermic ligand evaporation process. In the present case, the existence of a local minimum on the ground-state surface corresponding to an insertion complex of the form $H–MgNH_2^+$ may play an important role in such selectivity. The high selectivity for H-atom loss suggests that in the monomer, internal conversion to the ground state occurs for nuclear configurations in the vicinity of this complex. In fact, the observation that the H-loss channel is more selective in our studies, conducted with colder ions, suggests that a narrower range of favorable Franck-Condon factors populates the excited-state surface more selectively. Once insertion is initiated, the geometry is reminiscent of the hydrogen-atom migration mechanism discussed by Davis *et al.* on $Ba + CH_3OH$ and $Ba + H_2O$.[59] The $3s$ orbital of the ground state will greatly facilitate a H-atom migration because its spherical symmetry will overlap with the $1s$ orbital of H over the entire course of the reaction. Perhaps most importantly, the chromophore absorption shifts to the red with a larger cluster size, limiting the electronic energy of the complex and blocking access to the high-energy region of the surface in the vicinity of the insertion complex. Such a picture is consistent with our observation that while the ground-state H-loss channel readily occurs in a range of parent cluster sizes, by a metastable decay of vibrationally excited ground-state species, the photoinduced hydrogen-atom loss only occurs in the monomer. However, the limited data offered in support of this interpretation do not exclude the possibility of an excited-state decay. This issue clearly requires additional experimental and theoretical work.

As we noted previously, the branching ratios for solvent evaporation map out a more complex pattern than the mul-

tiple solvent loss governed by the available energy. For clusters with five, six, or seven solvents, the high-energy end of the dissociation spectrum is consistently dominated by the loss of two solvent molecules. However, in the hexamer and heptamer, the loss of three solvent molecules is the overwhelmingly favored loss channel in the range between 8000 and 10 000 cm^{-1}. In the hexamer, the monotonic growth of the $-2L$ channel with photolysis energy takes over beyond 11 000 cm^{-1}. In the heptamer, the selective evaporation of the three ligands near 8000 cm^{-1} gives over to the loss of both two and four solvent molecules above 10 000 cm^{-1}. These fragmentation patterns suggest that multiple isomers may be present in the cluster beam. In the absence of *ab initio* calculations of the geometries and transition moments for clusters with more than four solvent molecules, it is difficult to speculate on plausible dissociation mechanisms. However, theory does not predict significant transition moments for species in the $n=4$ spectrum of Fig. 2 below $\sim$16 400 cm^{-1}, where one might expect other isomeric species to absorb. The explanation of the anomalous branching ratios in the higher clusters clearly requires additional experimentation, possibly with infrared probes of ground-state species and theoretical treatments of the spectra and isomerization and dissociation processes occurring in these species.

CONCLUSIONS

The experiments reported here on the size dependence of the photodissociation signals for clusters of the form $Mg^+(NH_3)_n$, for $n=1$ to 7 complement and extend the existing work on this interesting system. The production of cold clusters has allowed sharp electronic origin bands to be observed, particularly for the lowest energy transitions in clusters with at least four solvent molecules. As predicted theoretically, clusters with four solvents adopt a low-energy configuration with tetrahedral symmetry, in which the electronic states based on the $3p$ orbitals of the core Mg^+ ion are quasidegenerate. The persistence of the resultant narrow absorption band in clusters with a second solvation shell provides evidence that the dominant geometry for these clusters is based on a tetrahedrally symmetric cluster core. The product branching ratios for the dissociation processes provide quantitative information on the electronic origins of excited states in small clusters and are also suggestive of the presence of multiple isomers of larger clusters. Understanding the latter issue requires additional experimental and theoretical work that will elucidate those structures and the processes leading to interconversion among isomeric forms. Of more global interest is the role that this system appears to play in developing a consensus that small polar solvent clusters based on one-electron cores can serve as models for the onset of spontaneous ionization and electron solvation. We look forward to continued experimental and theoretical progress in understanding the intermolecular interactions responsible for this behavior.

ACKNOWLEDGMENTS

The authors gratefully acknowledge the support of this work under National Science Foundation Grant No. CHE-095-23401. Acknowledgment is also made to the Donors of the Petroleum Research Fund, administered by the American Chemical Society, for the partial support of this research.

[1] A. J. Stace, Phys. Chem. Chem. Phys. **3**, 1935 (2001).
[2] A. J. Stace, J. Phys. Chem. A **106**, 7993 (2002).
[3] J. M. Farrar, Int. Rev. Phys. Chem. **22**, 593 (2003).
[4] P. D. Kleiber and J. Chen, Int. Rev. Phys. Chem. **17**, 1 (1998).
[5] M. A. Duncan, Annu. Rev. Phys. Chem. **48**, 69 (1997).
[6] C. S. Yeh, J. S. Pilgrim, K. F. Willey, D. L. Robbins, and M. A. Duncan, Int. Rev. Phys. Chem. **13**, 231 (1994).
[7] D. C. Sperry, A. J. Midey, J. I. Lee, J. Qian, and J. M. Farrar, J. Chem. Phys. **111**, 8469 (1999).
[8] J. Qian, A. J. Midey, S. G. Donnelly, J. I. Lee, and J. M. Farrar, Chem. Phys. Lett. **244**, 414 (1995).
[9] S. G. Donnelly, C. A. Schmuttenmaer, J. Qian, and J. M. Farrar, J. Chem. Soc., Faraday Trans. **89**, 1457 (1993).
[10] F. Misaizu, M. Sanekata, K. Tsukamoto, and K. Fuke, J. Phys. Chem. **96**, 8259 (1992).
[11] M. Sanekata, F. Misaizu, and K. Fuke, J. Chem. Phys. **104**, 9768 (1996).
[12] M. Sanekata, F. Misaizu, K. Fuke, S. Iwata, and K. Hashimoto, J. Am. Chem. Soc. **117**, 747 (1995).
[13] C. W. Bauschlicher, Jr., M. Sodupe, and H. Partridge, J. Chem. Phys. **96**, 4453 (1992).
[14] M. H. Shen and J. M. Farrar, J. Phys. Chem. **93**, 4386 (1989).
[15] S. G. Donnelly and J. M. Farrar, J. Chem. Phys. **98**, 5450 (1993).
[16] M. Sodupe and C. W. Bauschlicher, Jr., Chem. Phys. Lett. **195**, 494 (1992).
[17] C. Berg, M. Beyer, U. Ashatz, S. Joos, G. Niedner-Schatteburg, and V. E. Bondybey, Chem. Phys. **239**, 379 (1998).
[18] B. M. Reinhard and G. Niedner-Schatteburg, Phys. Chem. Chem. Phys. **4**, 1471 (2002).
[19] B. M. Reinhard and G. Niedner-Schatteburg, Phys. Chem. Chem. Phys. **5**, 1970 (2003).
[20] B. M. Reinhard and G. Niedner-Schatteburg, J. Chem. Phys. **118**, 3571 (2003).
[21] C. W. Bauschlicher, Jr. and H. Partridge, J. Phys. Chem. **95**, 3946 (1991).
[22] R. K. Milburn, V. I. Baranov, A. C. Hopkinson, and D. K. Bohme, J. Phys. Chem. A **102**, 9803 (1998).
[23] A. Andersen, F. Muntean, D. Walter, C. Rue, and P. B. Armentrout, J. Phys. Chem. A **104**, 692 (2000).
[24] M. Elhanine, L. Dukan, P. Maitre, W. H. Breckenridge, S. Massick, and B. Soep, J. Chem. Phys. **112**, 10912 (2000).
[25] S. Yoshida, N. Okai, and K. Fuke, Chem. Phys. Lett. **347**, 93 (2001).
[26] S. Yoshida, K. Daigoku, N. Okai, A. Takahata, A. Sabu, K. Hashimoto, and K. Fuke, J. Chem. Phys. **117**, 8657 (2002).
[27] D. E. Powers, S. G. Hansen, M. E. Geusic, D. L. Michalopoulos, and R. E. Smalley, J. Chem. Phys. **78**, 2866 (1983).
[28] W. C. Wiley and I. H. McLaren, Rev. Sci. Instrum. **26**, 1150 (1955).
[29] F. Misaizu, M. Sanekata, and K. Fuke, J. Chem. Phys. **100**, 1161 (1994).
[30] W. Lu and S. Yang, J. Phys. Chem. A **102**, 825 (1998).
[31] J. I. Lee and J. M. Farrar, J. Phys. Chem. A **106**, 11882 (2002).
[32] J. I. Lee, J. Qian, D. C. Sperry, A. J. Midey, S. G. Donnelly, and J. M. Farrar, J. Phys. Chem. A **106**, 9993 (2002).
[33] J. I. Lee, D. C. Sperry, and J. M. Farrar, J. Chem. Phys. **114**, 6180 (2001).
[34] O. M. Cabarcos, C. J. Weinheimer, and J. M. Lisy, J. Phys. Chem. A **103**, 8777 (1999).
[35] J. A. Draves, Z. Luthey-Schulten, W.-L. Liu, and J. M. Lisy, J. Chem. Phys. **93**, 4589 (1990).
[36] C. S. Yeh, K. F. Willey, D. L. Robbins, J. S. Pilgrim, and M. A. Duncan, J. Chem. Phys. **98**, 1867 (1993).
[37] K. F. Willey, C. S. Yeh, D. L. Robbins, J. S. Pilgrim, and M. A. Duncan, J. Chem. Phys. **97**, 8886 (1992).
[38] M. Sodupe and C. W. Bauschlicher, Jr., Chem. Phys. Lett. **212**, 624 (1993).
[39] C. W. Bauschlicher, Jr. and H. Partridge, J. Phys. Chem. **95**, 9694 (1991).
[40] C. W. Bauschlicher, Jr. and H. Partridge, Chem. Phys. Lett. **181**, 129 (1991).
[41] J. M. Lisy, Int. Rev. Phys. Chem. **16**, 267 (1997).
[42] P. J. Campagnola, D. J. Lavrich, and M. A. Johnson, J. Phys. (Paris), Colloq. **1**, 93 (1991).
[43] T. R. Tuttle and S. Golden, J. Phys. Chem. **95**, 5725 (1991).

[44] K. Fuke, K. Hashimoto, and S. Iwata, *Advances in Chemical Physics* (Wiley-Interscience, New York, 1999), Vol. 110, pp. 431–523.
[45] K. Hashimoto, T. Kamimoto, N. Miura, R. Okuda, and K. Daigoku, J. Chem. Phys. **113**, 9540 (2000).
[46] K. Hashimoto, T. Kamimoto, and K. Daigoku, J. Phys. Chem. A **104**, 3299 (2000).
[47] P. Brockhaus, I. V. Hertel, and C. P. Schulz, J. Chem. Phys. **110**, 393 (1999).
[48] K. Hashimoto, S. He, and K. Morokuma, Chem. Phys. Lett. **206**, 297 (1993).
[49] K. Hashimoto and K. Morokuma, J. Am. Chem. Soc. **117**, 4151 (1995).
[50] S. Nonose, T. Taguchi, K. Mizuma, and K. Fuke, Eur. Phys. J. D **9**, 309 (1999).
[51] S. Nonose, T. Taguchi, F. W. Chen, S. Iwata, and K. Fuke, J. Phys. Chem. A **106**, 5242 (2002).
[52] K. Daigoku, N. Miura, and K. Hashimoto, Chem. Phys. Lett. **346**, 81 (2001).
[53] R. Takasu, F. Misaizu, K. Hashimoto, and K. Fuke, J. Phys. Chem. A **101**, 3078 (1997).
[54] D. E. Clemmer and P. B. Armentrout, J. Phys. Chem. **95**, 3084 (1991).
[55] M. R. France, S. H. Pullins, and M. A. Duncan, Chem. Phys. **239**, 447 (1998).
[56] D. E. Clemmer and P. B. Armentrout, J. Am. Chem. Soc. **111**, 8280 (1989).
[57] K. Fuke, F. Misaizu, M. Sanekata, K. Tsukamoto, and S. Iwata, Z. Phys. D: At., Mol. Clusters **26**, S180 (1993).
[58] I. V. Hertel, in *Dynamics of the Excited State*, edited by K. P. Lawley (Wiley-Interscience, New York, 1982), Vol. L, p. 475.
[59] H. F. Davis, A. G. Suits, Y. T. Lee, C. Alcaraz, and J.-M. Mestdagh, J. Chem. Phys. **98**, 9595 (1993).